Fluctuating lift forces and pressure distributions due to vortex shedding in tube banks

K. C. Shim
Cipher Data Products International, Singapore

R. S. Hill
Formerly with University of Newcastle Upon Tyne, UK (deceased)

R. I. Lewis
Department of Mechanical Engineering, University of Newcastle Upon Tyne, UK

Received 12 January 1987 and accepted for publication 2 April 1987

Experimental measurements of fluctuating lift forces and surface pressure distributions are presented for staggered and in-line tube banks consisting of four rows, with transverse pitch-to-diameter ratio (P_T/d) of 2.67 and longitudinal pitch-to-diameter ratio (P_L/d) of 2.31. A strain gauge system was used to measure the fluctuating force on one instrumented tube located at various positions in the tube banks. A second instrumented tube was equipped with a static pressure tapping and a pressure transducer to provide time average and rms fluctuating surface pressure distributions, respectively. Investigations of the staggered tube bank revealed that the highest levels of fluctuating lift coefficients occurred in the second row. For the in-line geometry, on the other hand, similar levels of fluctuating lift coefficient were found in the second, third, and fourth tube rows. The normal configuration for staggered tube banks as used here is symmetrical. Further tests were undertaken for an asymmetric geometry, revealing a major reduction in the fluctuating lift forces as compared with symmetrical geometry. It is concluded that the use of irregular geometries in staggered tube banks should be further investigated as a practical solution to the reduction of vortex-induced vibrations in tubular heat exchangers.

Keywords: vortex street; tube bank; heat exchanger

Introduction

During the postwar period, as major advances have been made in thermal power systems, mechanical failures due to tube vibrations in heat exchangers have been a cause for serious concern to designers. This has led to many investigations of fluid dynamically induced vibrations, mainly conducted on tube banks. Unfortunately only a few of these studies have actually involved the measurement of the fluctuating forces or surface pressures, the main reason being the difficulties in devising suitable measuring techniques which are nonintrusive and can be accommodated within the compact geometry of a tube bank. One main objective of the present project was to develop such techniques.

The fluctuating lift coefficient due to vortex shedding from a single cylinder has been measured by many workers, including Tritton,[1] Humphreys,[2] Keefe,[3] Fung,[4] Schmidt,[5] McGregor,[6] and Kacker, Pennington, and Hill.[7] However their results for this simplest of all geometries show considerable scatter so that no precise correlation could be established. Hill[7] has also shown the importance of aspect ratio (cylinder length/diameter) in wind tunnel tests for single cylinders, establishing that, for aspect ratios less than 2.0, vortex shedding is likely to be correlated sufficiently along the cylinder for conditions to be considered to be two-dimensional. However, predictions of rms lift by the vortex cloud method are in excess of the "two-dimensional" experimental values by a factor of about 58% according to Lewis and Shim.[8] In this reference the authors also reported significant differences between experimental and measured surface pressure fluctuations for the fairly high aspect ratio of 6.0 used in the present project. These differences implied the possibility of instabilities in the vortex street along the length of each shed vortex, i.e., parallel to the length of the tube, the effects of which are generally favorable, leading to reduced surface pressure fluctuations and thus less excitation. However, there may be an associated specific mode of vibration associated with this phenomenon, which is in need of further investigation. Thus, although much is already known about vortex shedding fluctuations for single cylinders, there is still much work to be done, related in particular to three-dimensional effects.

In view of the additional complexity of the flow in tube banks, it is not surprising that there has been no equal volume of experimental measurements of fluctuating forces and pressures, so comparative information is scarce. One of the few comprehensive studies of fluctuating lift forces in tube bundles was conducted by Chen,[9] using both in-line and staggered tube banks, with several combinations of transverse and longitudinal spacings. Unfortunately, only one selected tube in the middle of the tube bundle was taken to measure the lift forces for each tube bank configuration. Although it was admitted that the results were limited and of low accuracy, Chen was able to show that for a fixed transverse spacing the fluctuating lift coefficient increased with increases in longitudinal spacing. However, comparisons of fluctuating lift coefficients between the different rows of a given tube bank configuration were not investigated. In view of this, such measurements were given priority in the present investigation.

The literature on surface pressure distributions in tube banks

is, surprisingly, equally scarce, Batham[10] being one of the few research workers to carry out experimental measurements on both average and fluctuating pressures. His investigations were carried out on in-line tube banks having P_T/d and P_L/d ratios of 2:1 and 1.25:1, respectively, over the Reynolds number range of 2.8×10^4 to 1.0×10^5. Batham found that Re had negligible effect upon the mean and fluctuating pressure coefficients.

Although pragmatic solutions are available to damp down vortex-induced vibrations in heat exchanger engineering practice, it is regretted that fundamental knowledge of underlying excitation mechanisms and ongoing related research is so limited. The purpose of the present research project was to fill some of the gaps revealed by the above brief review by carrying out experimental investigations of fluctuating lift forces due to vortex shedding in both staggered and in-line tube banks. Measurements of time averaged and fluctuating pressures were also carried out to provide supporting evidence and additional information. In each of the three tube banks investigated, one instrumented tube was introduced successively into each of the four tube rows. The instrumented tube for measuring fluctuating lift force was flexibly mounted, the remaining neighboring tubes being modeled by rigid wooden rods. For pressure measurements the second instrumented tube was used instead and was rigidly mounted. Details of this equipment will be given in the next section, followed by an outline of the experiments and results in subsequent sections.

Test equipment and experimental methods

In the following subsections we shall briefly outline the wind tunnel tube bank configurations, the force measuring system,

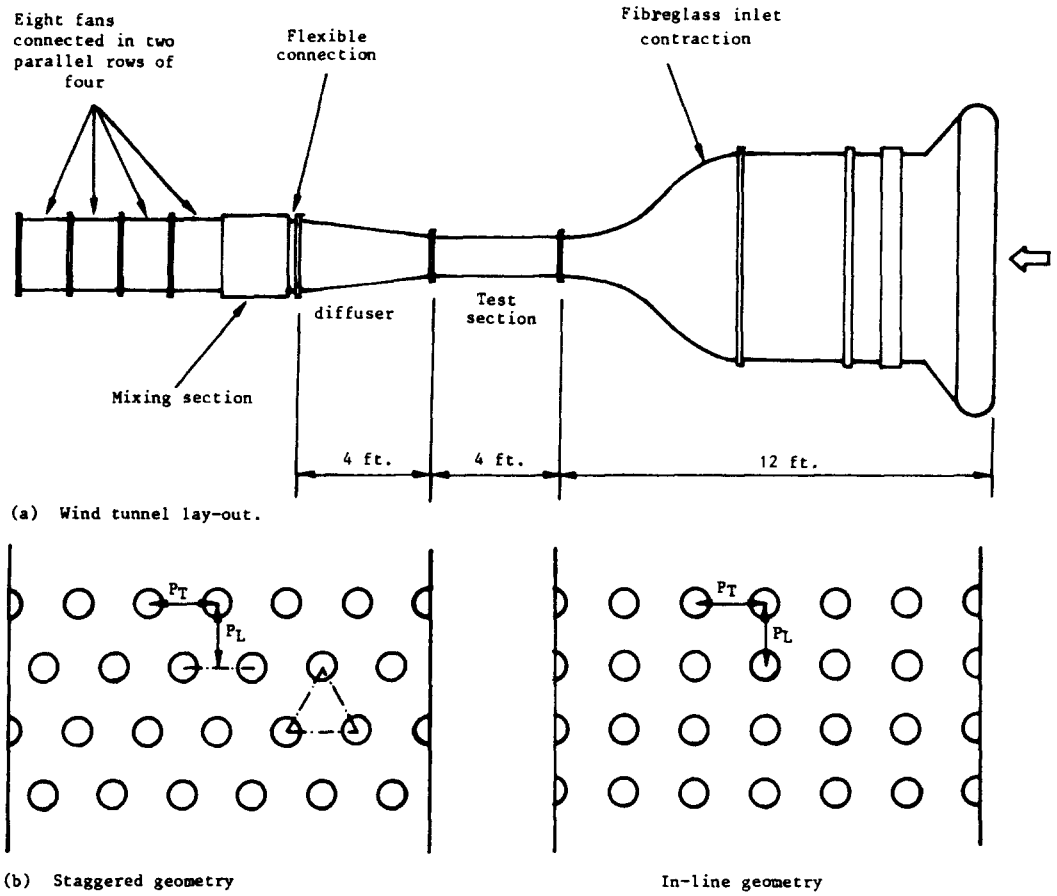

Figure 1 Open-circuit wind tunnel and tube bank geometries

Notation

A_v	Amplitude of vibration
C_p	Time averaged surface pressure coefficient
C'_p	Rms fluctuating surface pressure coefficient
C_L	Rms lift coefficient
d	Tube diameter
f_v	Vortex shedding frequency
L	Lift force
L_{rms}	Rms lift force
p	Static pressure
p_{av}	Time averaged static pressure
p_∞	Static pressure upstream of tube banks
P_T	Transverse pitch of tubes
P_L	Axial pitch of tube rows
Re	Reynolds number Ud/v
S	Strouhal number $f_v d/U$
t	Time
U	Mainstream flow velocity upstream of tube banks
U_g	Mean flow velocity in gap $= U/(1-d/P_T)$
ρ	Density
v	Kinematic viscosity

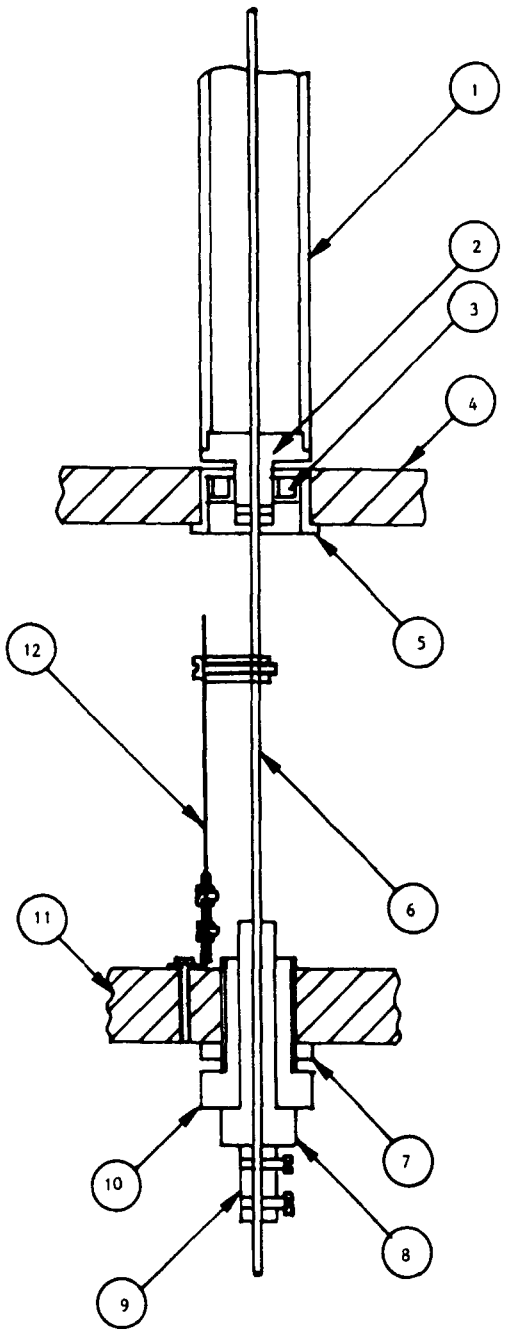

1. Perspex tube
2. Aluminium end cap
3. Silicon rubber seal
4. Lower tunnel wall
5. Seal support
6. Piano wire (0 = 0.064" dia.)
7. Locking nut
8. Shoulder guide
9. Locking device for piano wire
10. Adjusting bolt
11. Metal frame support
12. Thin metal strip with strain gauges

Figure 2 Detailed view of the instrumental tube for force measurement

and the instrumented cylinder for surface pressure measurements.

Wind tunnel tube bank configurations

All experiments were carried out in the test section of an open-circuit wind tunnel illustrated in Figure 1(a) and more fully described by Pennington[11] and Shim.[12] The test section was 24 in. wide, 9 in. high, and 48 in. long. Both sidewalls were made of perspex to facilitate visual alignment of probes and were removable to allow access to the tube banks or instrumentation during tests. The top and bottom walls were constructed from blockboard, with mounting holes drilled in accordance with the requirements for diameter and spacing of the various tube arrays. Rigidly mounted wooden rods of $1\frac{1}{2}$ in. diameter were used to simulate the heat exchanger tubes, any of which could be removed as required to accommodate either of the instrumented tubes. The two main tube bank geometries investigated are illustrated in Figure 1(b), one being symmetrically staggered and the other in-line. Both consisted of four rows with transverse spacing-to-diameter ratios of $P_T/d = 2.67$ and longitudinal spacing-to-diameter ratios of $P_L/d = 2.31$.

The force measuring system

The design objective was to provide a means for measuring the total fluctuating force experienced by a single tube at one selected location within the tube bank, the tube being able to move against an elastic restraint. Strain gauges could then be used to measure the tube displacement and, hence, by calibration, the imposed instantaneous aerodynamic force.

The solution to this requirement adopted here is illustrated in Figure 2. The elastic restraint was provided by a piano wire

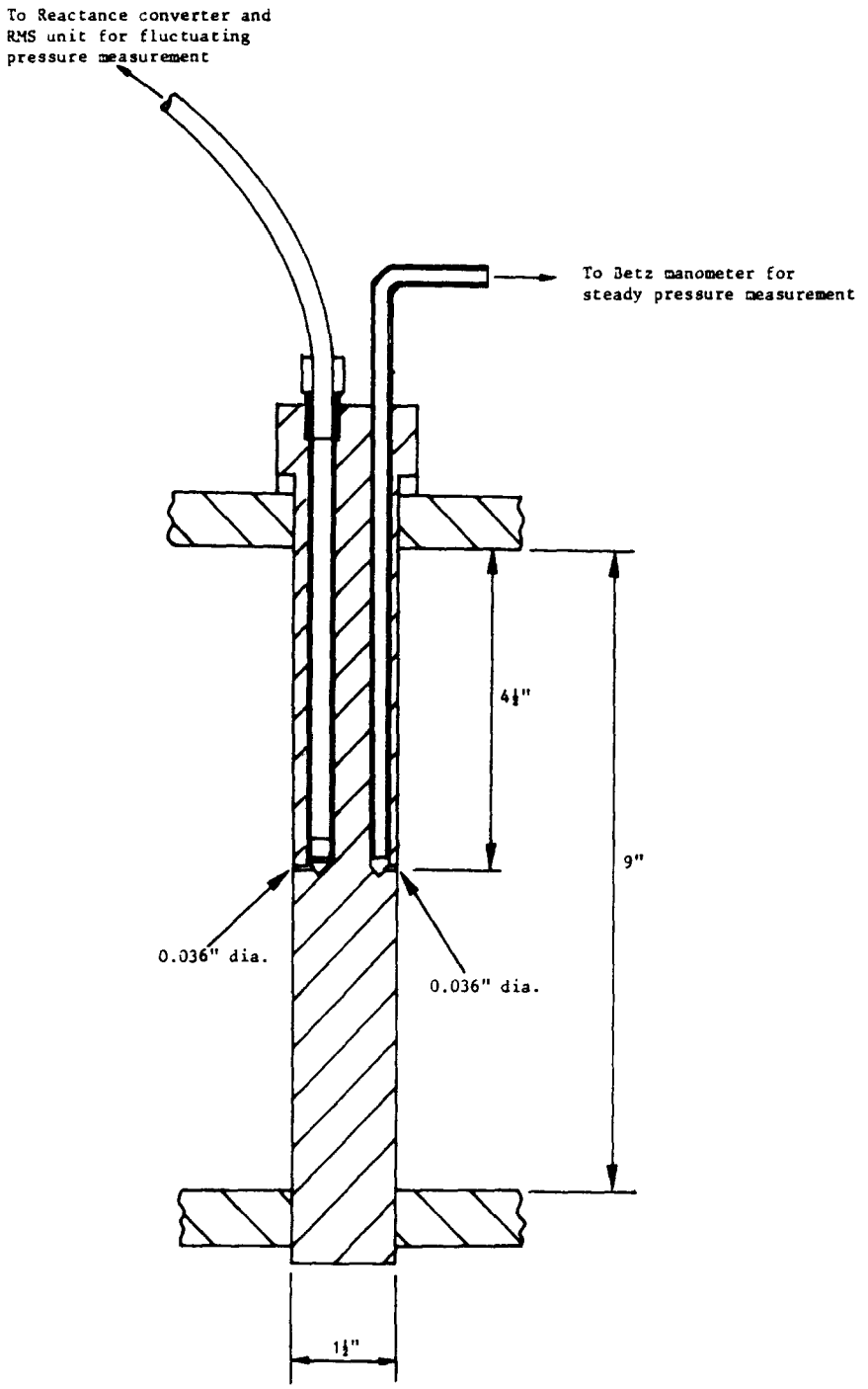

Figure 3 Instrumented tube for surface pressure measurement

21 in. long fixed to pretensioning points on a rigid steel frame which surrounded the working section. As shown in Figure 2, the tube, which was made of perspex, was fixed to the wire with end caps, transferring the aerodynamic forces directly to the wire. Displacement of the tube was transmitted to a thin flexible metal strip of dimensions 4.5 in. × 0.5 in. × 0.015 in., which offered negligible elastic restraint. A pair of strain gauges was fixed on opposite sides of the metal strip to provide temperature compensation as well as increased sensitivity. Strain gauge output was related to the force experienced by the tube in a calibration procedure described in Ref. 12.

In selecting a force measuring system based upon tube displacement against an elastic restraint, two important factors must be considered: the natural frequency of the measuring system and the amplitudes of vibration likely to be encountered by the measuring system. The elastic tube mounting was not intended to simulate tube stiffness but only to provide the means for measurement. It was important therefore that the first natural frequency of the measuring system should be greater than the dominant frequencies of the fluctuating aerodynamic force on the tube. To obtain strong signals this margin should be kept as small as possible. On the other hand, if the force fluctuations approach or exceed this first resonant frequence, the response of the measuring system is no longer

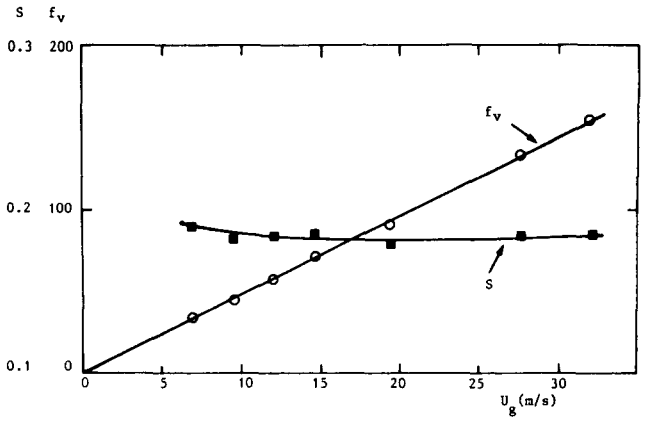

Figure 4 Graphs of vortex shedding frequency f_v and Strouhal number S versus U for a single tube in crossflow

linear. The design of the measuring system in such circumstances is extremely difficult since its sensitivity is strongly frequency dependent. Furthermore it imposes an effective upper limit upon mainstream flow velocities and, therefore, Reynolds numbers which may be investigated. On the other hand, a measuring system of needlessly high natural frequency will result in small amplitudes of response and therefore demand high amplification. By adjusting the piano wire tension it was possible to arrive at a compromise value of 80 Hz for the natural frequency of the measuring system, which was normally acceptable for wind tunnel velocities up to 14 m/s.

Instrumented cylinder for pressure measurements

The instrumented cylinder used for measuring surface pressure distributions is shown in cross section in Figure 3. This cylinder, which spanned the 9-in. dimension of the wind tunnel, could be rotated through 360° and was provided with holes at mid-height for independent measurement of the average and rms fluctuating pressures. One static tapping was directly connected to a Betz manometer for estimation for the average static pressure. The other pressure tapping, used for measurement of rms fluctuating pressures, opened into a 3/8-in.-diameter hole, into which was inserted a pressure transducer probe. The transducer, mounted at the end of the probe, was a Bruel and Kjaer type with a 0.25-in.-diameter condenser microphone, connected through an oscillator, reactance converter, and rms unit to give finally the rms pressure as output. The definitions of average and rms fluctuating pressure coefficients are as follows.

The time averaged pressure coefficient is defined as

$$C_p = \frac{p_{av} - p_\infty}{\frac{1}{2}\rho U^2} \tag{1}$$

where for a period of time t_1 to t_2 the average pressure is given by

$$p_{av} = \frac{\int_{t_1}^{t_2} p \, dt}{t_2 - t_1} \tag{2}$$

p_∞ is the static pressure in the working section just upstream of the tube bank, and U is the mainstream velocity at this location.

The rms fluctuating pressure coefficient is defined as

$$C'_p = \frac{1}{\frac{1}{2}\rho U^2} \sqrt{\left[\frac{\int_{t_1}^{t_2} (p - p_{av})^2 \, dt}{t_2 - t_1}\right]} \tag{3}$$

In addition, we may also define an rms lift coefficient

$$C_L = \frac{L_{rms}}{\frac{1}{2}\rho U^2 d} \tag{4}$$

where the rms lift force is given by

$$L_{rms} = \sqrt{\left[\frac{\int_{t_1}^{t_2} L^2 \, dt}{t_2 - t_1}\right]} \tag{5}$$

Other instruments used in this investigation were hot wire anemometers and a Hewlett-Packard frequency analyzer. Discussions of other aspects of this experimentation have been given in Ref. 8 (average and fluctuating pressures for a single cylinder compared with vortex cloud theory) and Ref. 13 (the detection of vortex patterns using hot wire anemometer correlations of fluctuating velocity).

Experimental investigations

Early in this project experiments were carried out on a single tube as a preliminary check upon the feasibility of the force measuring system and the other instrumentation and to provide comparisons with previous research by other force measuring techniques. Following investigation of the symmetrically staggered and in-line tube banks, a final study was completed of the staggered tube bank with row No. 3 transversely offset by 1 in. to destroy symmetry and thereby affect the vortex shedding pattern. The experimental results may therefore be classified into four groups as follows. Each classification is discussed in the subsequent subsections:

(i) Single tube
(ii) Symmetrically staggered tube bank
(iii) In-line tube bank
(iv) Modified staggered tube bank with offset third row

Single tube

By frequency analysis of the hot wire anemometer, the vortex shedding frequency and, hence, the Strouhal number were evaluated for flow past the single instrumented tube over the velocity range 5.3 to 30.4 m/s, and are shown in Figure 4. As expected, the Strouhal number was almost constant and of average value 0.19, which agrees well with published results. The power spectral analyses of the lift force obtained from the strain gauge measuring system are shown in Figure 5 for several wind tunnel airspeeds. These reveal that the tube vibrations responded at two principal frequencies. One of these was clearly caused by the vortex shedding process, as its frequency varied linearly with U in accordance with Figure 4. The other peak in the power spectral analysis curve was due to the vibration of the measuring system at its own natural frequency of 80 Hz, a response which would result from the presence of any broadband turbulent excitation. As will be observed from Figure 5, the two excitation peaks merged at a wind tunnel speed of about 16 m/s, rising to an enormous amplitude as the system was excited due to the vortex street coinciding with its natural frequency. This is confirmed by the plot of arbitrary vibration amplitude at 80 Hz (i.e., the amplitude of the peak millivolt reading taken from the power spectrum displayed by the frequency analyzer) versus U shown in Figure 6.

A curve of C_L versus Reynolds number derived from these tests is shown in Figure 7 in comparison with the results of Humphreys,[2] Keefe,[3] Chen,[14] and Gerrard.[15] Because of the natural response of the system as just discussed, linearity was lost for wind tunnel speeds above, say, 13 m/s, which limited the comparisons shown here to a maximum Reynolds number of 3.3×10^4. The present results show best agreement with those of Gerrard, and they indicate a significant increase of C_L over the Reynolds number range 1.8×10^4 to 3.3×10^4.

Viewed overall, the results obtained for the single tube tests

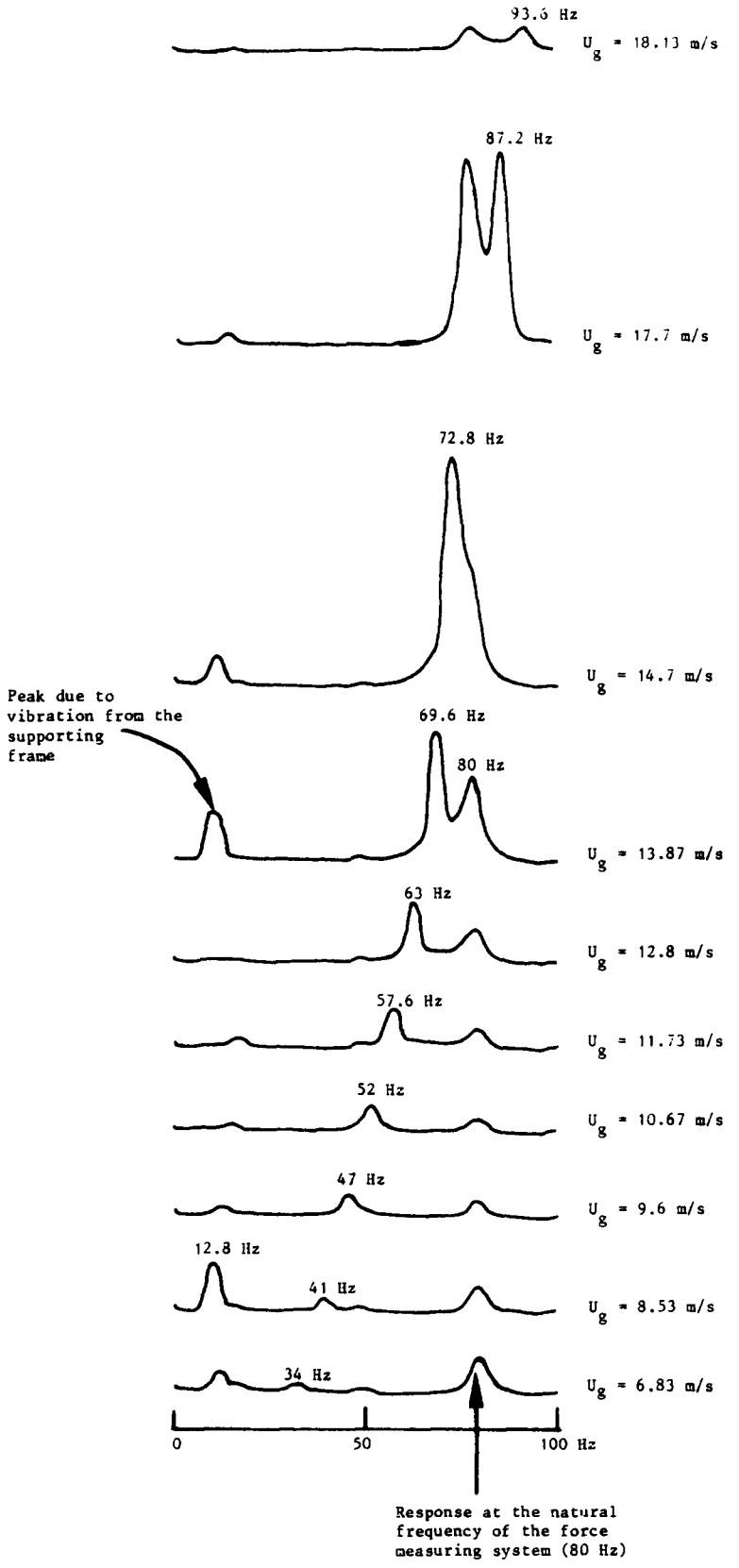

Figure 5 Vibration power spectra for a single tube in crossflow

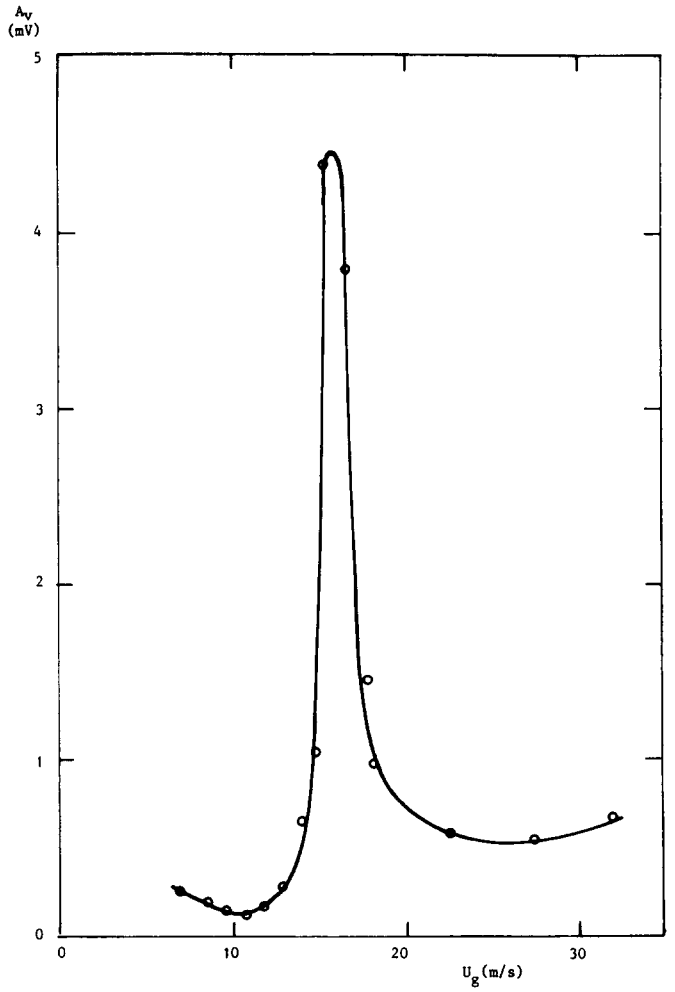

Figure 6 Plot of arbitrary vibration amplitude A_V at 80 Hz versus U for a single tube in crossflow

agreed sufficiently well in several respects with accepted published work for it to be safe to conclude that the force measuring system and instrumentation were suitable and performing satisfactorily.

Staggered tube bank

In the symmetrically staggered tube bank, hot wire measurements revealed the presence of two dominant frequencies in the velocity power spectra. In Refs. 12 and 13, where full discussions of these results are presented, it is concluded that two possible fluctuating flow phenomena were generated in the tube bank of separate origin. The fluctuation of lower frequency was certainly caused by a von Kármán-type vortex shedding process, but the nature of the higher-frequency fluctuation was uncertain. It was thought possibly to result from oscillation of the jet flow emerging from row 2 impinging upon the tubes of row 3. Some of these results are shown in Figure 8 for measurements undertaken with the hot wire probe positioned close to the middle tube of row 2 just outside the boundary layer at position x. The power spectral curves shown in Figure 8 clearly indicate the presence of two distinct frequency peaks produced by these two fluctuating phenomena. This is further highlighted in Figure 9, in which the peak frequencies and associated Strouhal numbers have been replotted against gap velocity U_g. Bearing in mind the relatively wide spacing ratios, we can reasonably conclude that the lower-frequency phenomenon, having an almost constant Strouhal number of 0.2, was caused by vortex street shedding. Flow visualization tests using smoke under stroboscopic illumination confirmed this, and is more fully described in Refs. 12 and 13, which also conclude, from hot wire velocity correlation analysis, that the vortex shedding patterns among the four rows exhibited remarkable behavior, as illustrated by Figure 10.

In the present investigations further evidence of the presence of two fluctuating flow phenomena was obtained from the response of the force measuring instrumented tube. Shown in Figure 11 are the arbitrary vibration amplitudes at 80 Hz measured with instrumented tubes placed in each of the four rows, for the wind tunnel speed range 6.0 to 25.0 m/s. These results clearly demonstrate that the instrumented tubes (all set to the same natural frequency of 80 Hz) responded to two velocity-dependent fluctuating flow phenomena. The instrumented tubes in each row would respond to narrowband excitation, such as that induced by vortex shedding, and to their natural frequencies under the influence of wideband excitation, such as that caused by a generally turbulent field. As the flow velocity U_g was increased from 6.0 m/s, so the first narrowband velocity-dependent excitation frequency increased, reaching 80 Hz at a gap velocity of $U_g = 10.05$ m/s (Figure 11). At this condition all four instrumented tubes responded strongly at their natural frequency of 80 Hz, indicating the certain presence of a fluctuating flow phenomenon with a Strouhal number of about 0.3. As the wind tunnel velocity was further increased to $U_g = 15.5$ m/s, the second response at 80 Hz of the four instrumented tubes occurred, in this case at a Strouhal number of 0.2, clearly due to vortex shedding.

With the knowledge that the lower-frequency fluctuating phenomenon was definitely a vortex shedding process, the relationships between the rms lift coefficient C_L and gap velocity U_g were determined for the velocity range below excitation, $U_g = 6.0$ to 12.3 m/s, and these are shown in Figure 12. These results show that the second row experienced the highest C_L level, followed by the third and fourth rows. The first row experienced negligible lift forces. The likely reason for the differences in C_L levels between the various rows in this symmetrically staggered configuration can be explained by the

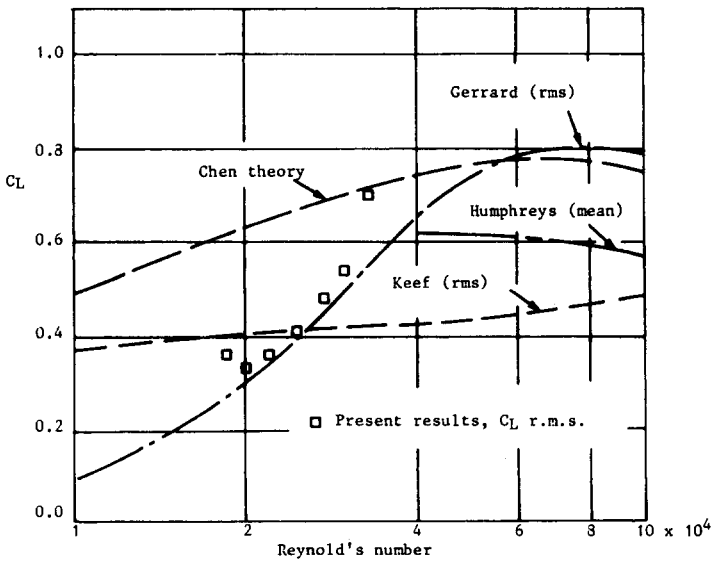

Figure 7 Flucutation lift coefficient C_L as a function of Reynolds number for a single tube in crossflow

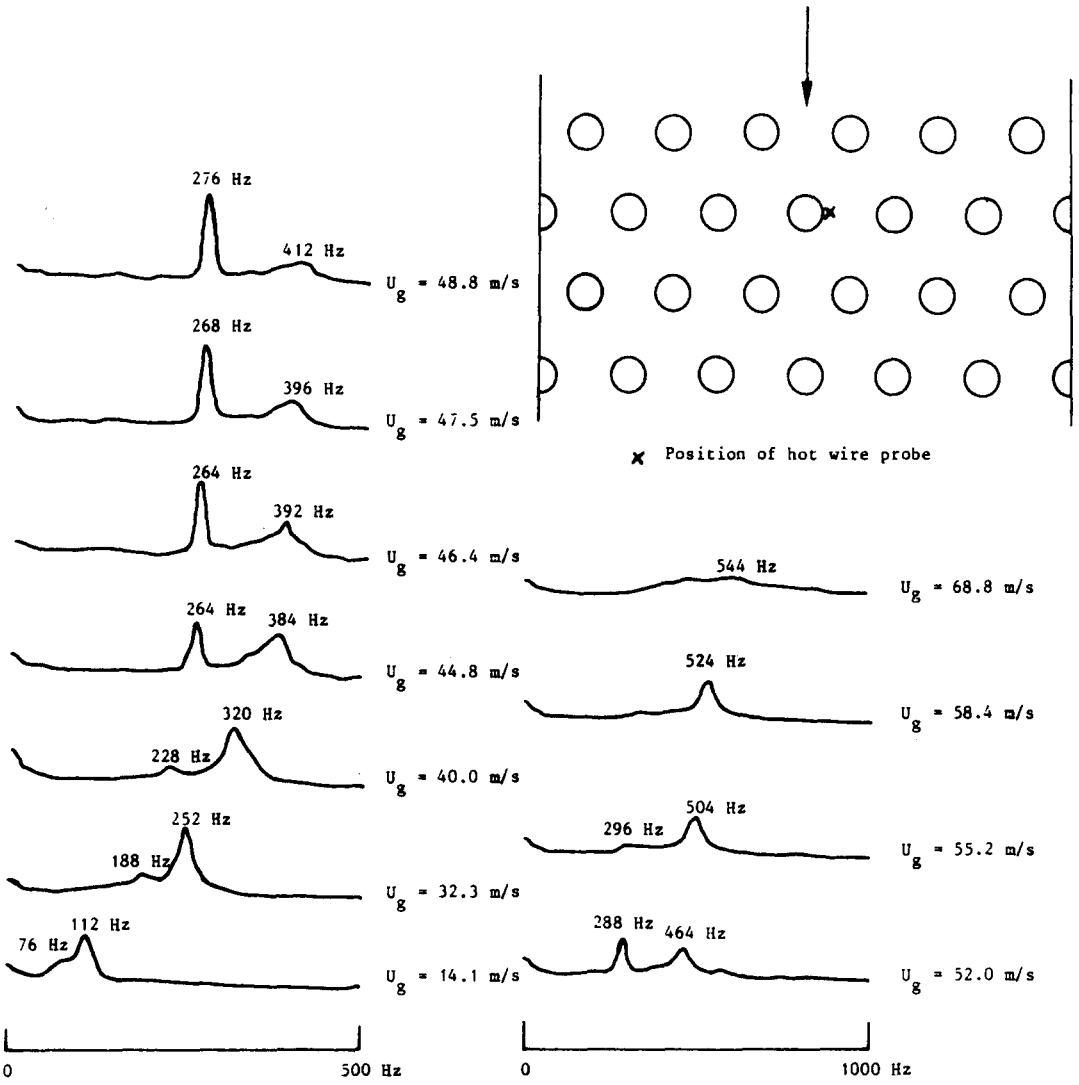

Figure 8 Velocity power spectra for staggered tube bank of four rows with P_T/d=2.67 and P_L/d=2.31. Hot wire position in the second row marked by x

occurrence of the different vortex shedding patterns as illustrated in Figure 11 and referred to earlier. We see that only the second and fourth rows shed oscillating von Kármán-type vortex streets. Row 1 sheds pulsating but symmetrical vortices from opposite sides, resulting in negligible rms lift coefficients. Row 2, the first row to shed true vortex streets, is subject to extremely large C_L values rising from 0.6 to 1.0. Because row 3 is also attempting symmetrical vortex shedding in a similar manner to row 1, we might expect a major reduction in C_L. In fact, this was not observed, presumably because of the progressive development of random turbulence of a large scale, which would lead to the growth of asymmetries by row 3. The excitation of row 4 due to vortex street shedding, however, seemed to still dominate despite the increasing effect of the disturbing turbulent eddies from upstream, judging by the large C_L values measured in that row.

The average and fluctuating pressure distributions for the center tube of each row are shown in Figures 13 and 14. As Figure 13 shows, the separation points were located at angular positions of about 90° and 80° from the leading edge point for rows 1 and 2 and were effectively uninfluenced by the Reynolds number. Note that the wake pressure distribution for row 2, which was shedding a vortex street, was quite similar to that of an isolated circular cylinder, as reported by Lewis and Shim,[8] in both shape and level. On the other hand, the wake static depression for row 1 was considerably less, indicating a reduction of vorticity production and energy dissipation for this symmetrical pulsating type of wake flow illustrated by Figure 10.

Proceeding to rows 3 and 4, however (Figure 13), separation was less distinct, probably due to the increasing level of large-scale turbulence from rows 1 and 2, which would cause the separation point to fluctuate a good deal. Row 4 showed considerable sensitivity to Reynolds number for reasons which are unknown. At the lower Reynolds number of 15,278 the wake static pressure was considerably reduced, possibly due to more coherent vortex street formation with greater viscous diffusion from the eddies emanating from upstream.

The fluctuating pressure distributions shown in Figure 14 are especially interesting. Row 1 exhibited almost uniform distributions of C'_p around the tube perimeter, suggesting a global pulsating effect caused by the symmetrical vortex shedding in the wake. In the second row, on the other hand, C'_p shows a distinct peak just upstream of the separation point at

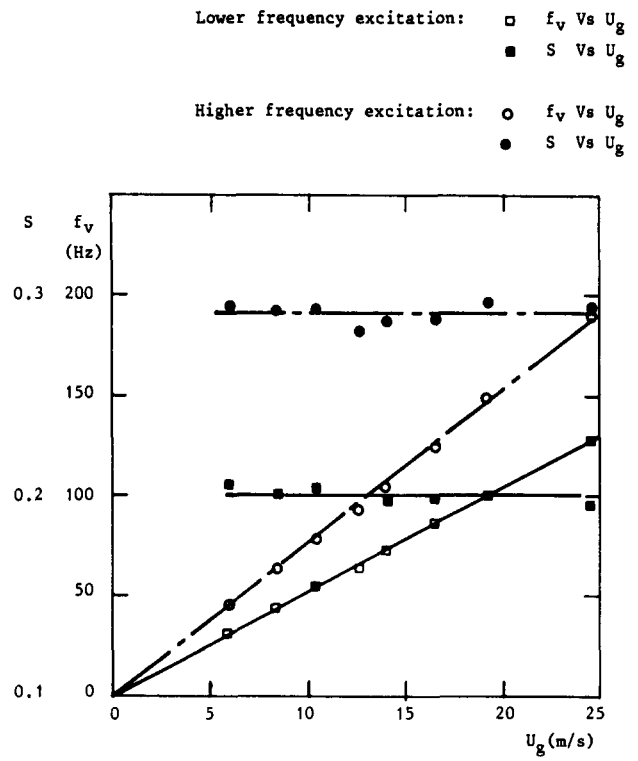

Figure 9 Graphs of f_v and S versus U_g for staggered tube bank of four rows with $P_T/d=2.67$ and $P_L/d=2.31$ in the U_g range between 0 and 25.0 m/s

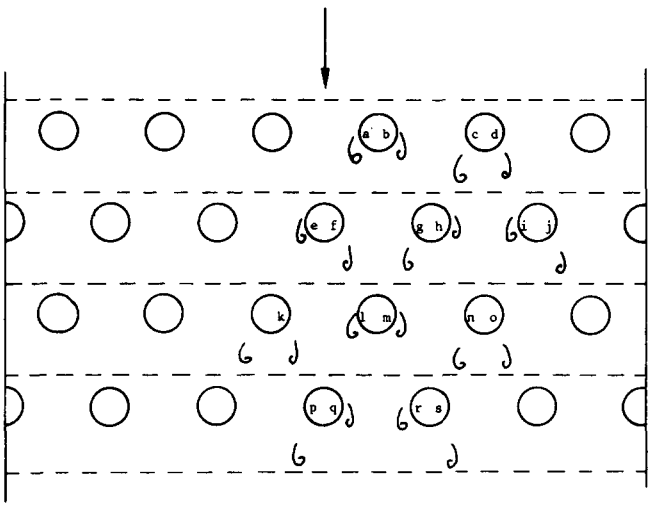

Figure 10 Simulated shedding pattern of vortex shedding in the staggered tube bank of four rows with $P_T/d=2.67$ and $P_L/d=2.31$. $U_g=8.32$ m/s

$\theta=70°$ and relatively constant levels downstream of this in the wake. In a previous paper Lewis and Shim[8] recorded the same behavior for unsteady fluctuating pressures downstream of separation for a single cylinder, disagreeing with theoretical predictions obtained by the two-dimensional vortex cloud method. According to the latter (so far not available for tube banks), C_p' increased to much larger proportions for the surface downstream of separation in the region closest to the von Kármán vortices, where one would indeed expect to measure the maximum fluctuations. It seems likely therefore that the vortex sheets undergo some form of instability in the third

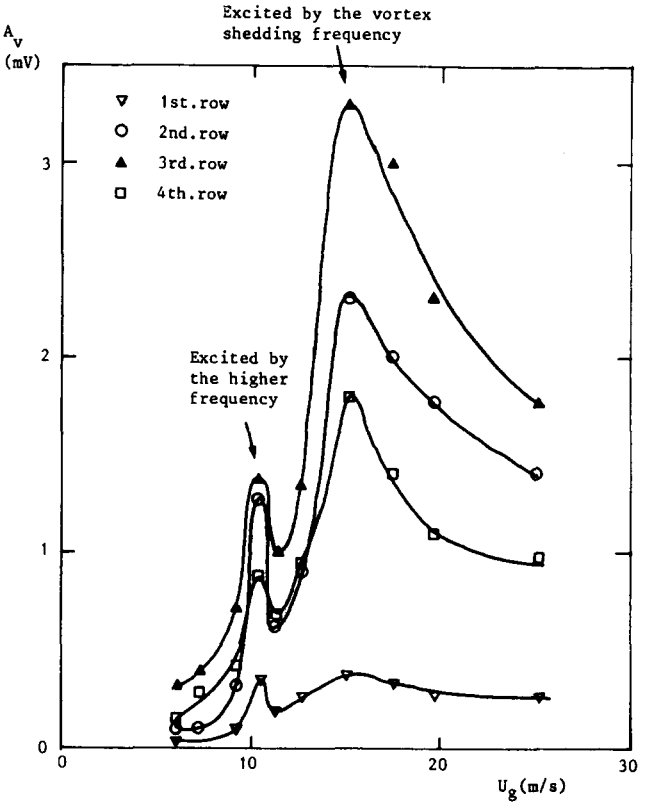

Figure 11 Graph of arbitrary vibration amplitude A_v at 80 Hz against U_g for staggered tube bank of four rows with $P_T/d=2.67$ and $P_L/d=2.31$

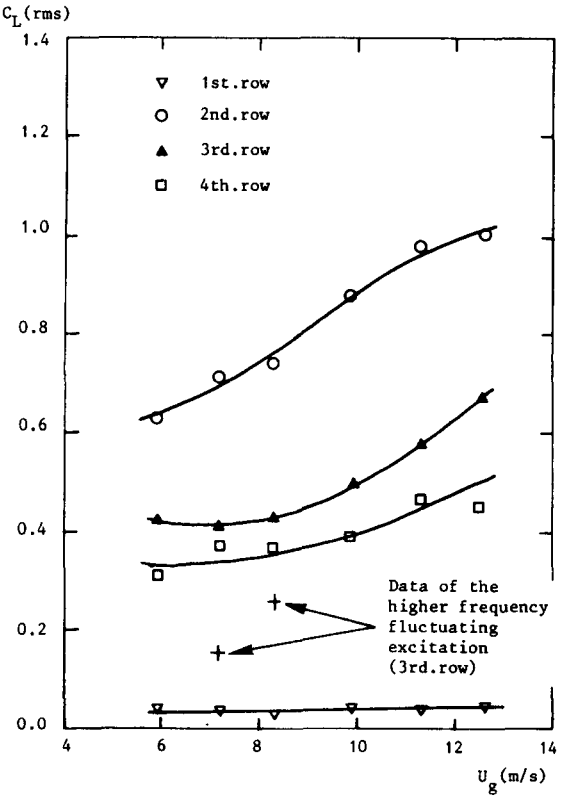

Figure 12 Graph of rms value of the total lift coefficient C_L versus U_g for staggered tube bank of four rows with $P_T/d=2.67$ and $P_L/d=2.31$

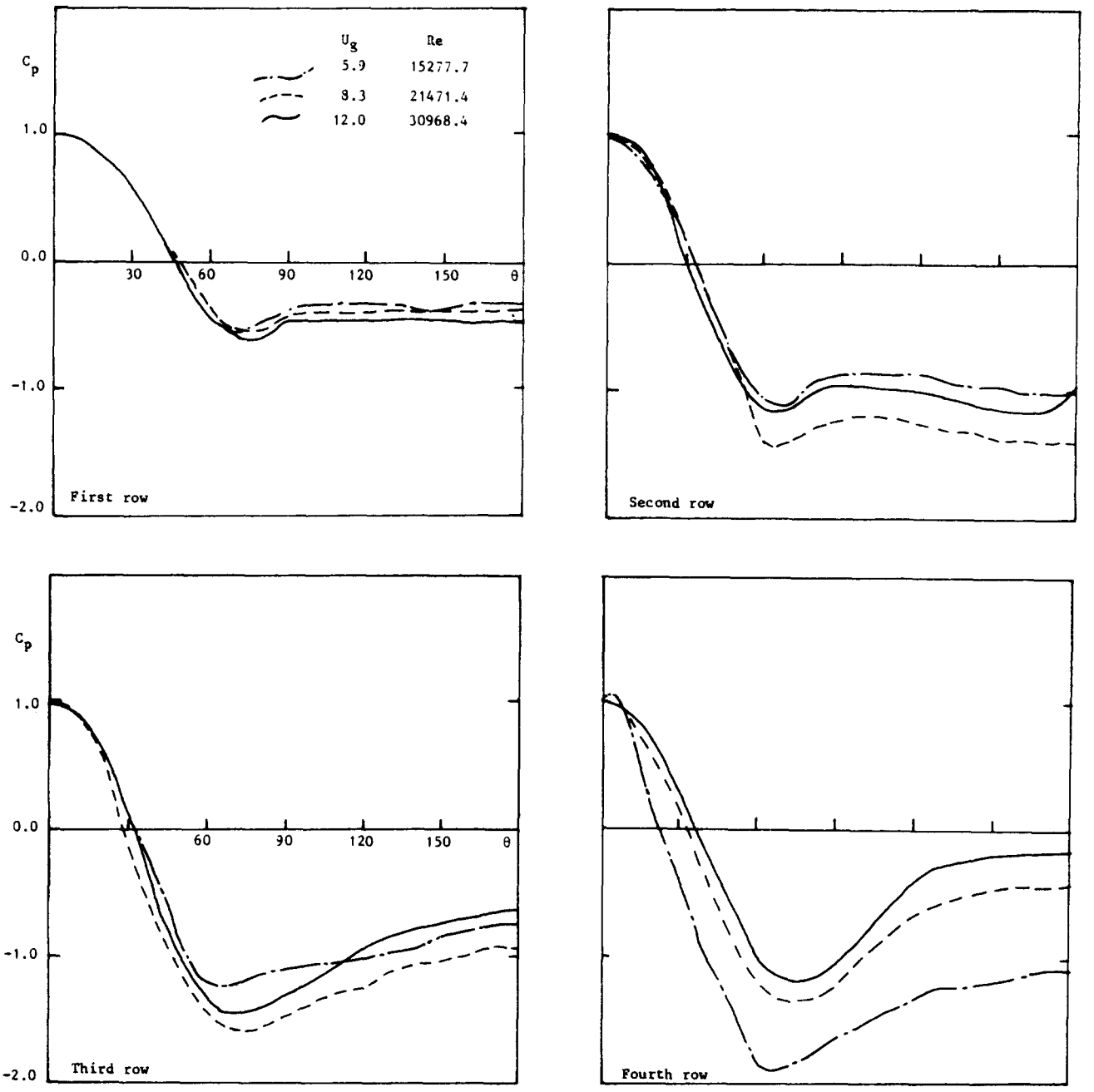

Figure 13 Steady pressure distribution for staggered tube bank of four rows with $P_T/d=2.67$ and $P_L/d=2.31$

dimension (i.e., parallel to the tubes) as they form into von Kármán eddies, resulting in a redistribution of the velocity fluctuations from two to three dimensions. The experimental measurements for row 2 shown here certainly support this hypothesis.

Proceeding to the fluctuating pressure plots for rows 3 and 4 (Figure 14), one can observe an increasing level of C'_p on the forward facing surface well upstream of the anticipated region for separation (e.g., $\theta<30°$). Undoubtedly this is the consequence of turbulent bombardment from the wakes leaving rows 1 and 2, resulting even in the production of a C'_p peak close to the upstream stagnation point (at $\theta=0°$ for row 3 and at $\theta=25°$ for row 4). Second peaks were produced closer to the likely separation region ($\theta=60°$ and $\theta=80°$ for row 4). Downstream of this, however, the fluctuating pressures tended to decay in both tube rows, particularly at the higher Reynolds numbers, indicating a progressive breakdown in scale and intensity of turbulence as the flow proceeds through the tube bank. All of this behavior follows the trend which one would expect with the one exception already mentioned, namely the absence of strong peak fluctuations close to the von Kármán vortices in rows 2 and 4. Comparing the C'_p plots for rows 3 and 4, however, one may perhaps notice some evidence of this in the shape, location, and wider spread of the second peak.

One worrying feature of the fluctuating pressure plots is their apparent sensitivity in overall level to the Reynolds number. For row 1, subject to negligible turbulent influences from upstream, this is markedly so and demands further investigation. The increase in C'_p level with reducing Reynolds number is manifest also for rows 2, 3, and 4 but to a reduced extent. Since C'_p was

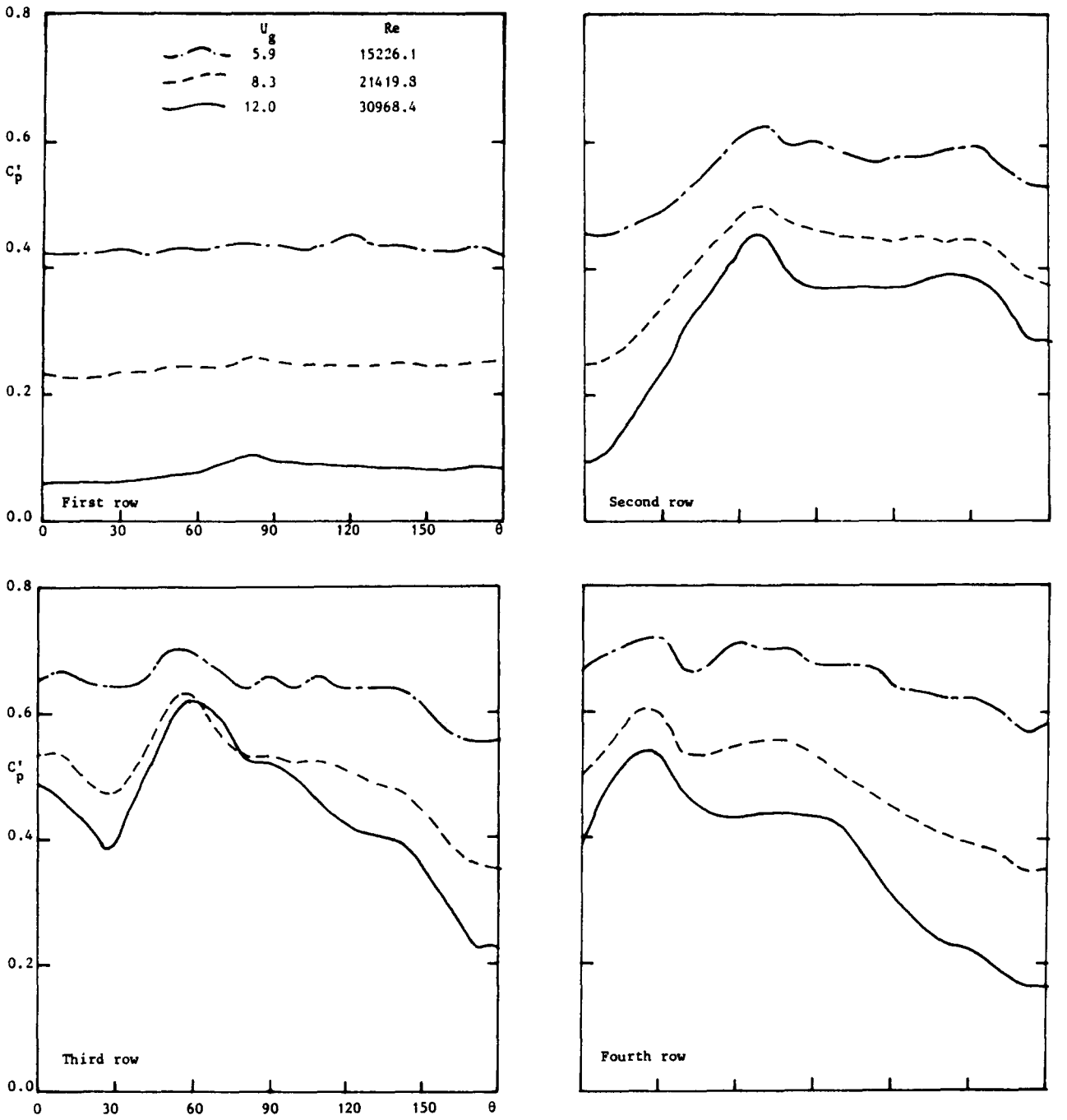

Figure 14 Fluctuating pressure distribution for staggered tube bank of four rows with P_T/d=2.67 and P_L/d=2.31

given directly by electronic means, there is no possibility for rechecking these results short of repeating the experiments. However, the trend is, as one might expect, for a form of fluid dynamic instability involving boundary layer separation from smooth surfaces at low Reynolds number and large-scale periodic eddies. It is possible that 0.15×10^5 to 0.3×10^5 represents a critical tube bank Reynolds number range in which separation and vortex sheet stability are sensitive to small changes of Reynolds number in the absence of mainstream turbulence. This would explain the particular behavior of row 1. Referring back to Figure 13, note that average pressures are far less sensitive to Reynolds number than are fluctuating pressures.

In-line tube bank

The hot wire measurements reported in Ref. 13 revealed only one dominant frequency and an associated vortex shedding pattern as illustrated in Figure 15, the Strouhal number being about 0.15. To provide further information about this, measurements were made of the rms lift coefficient and of average and fluctuating pressure distributions for the in-line tube bank case. The results are shown in Figures 16 to 18.

Curves of C_L versus U_g are shown in Figure 16 for all four tube rows, having the same P_T/d and P_L/d ratios as the staggered geometry, namely 2.67 and 2.31, respectively. If the

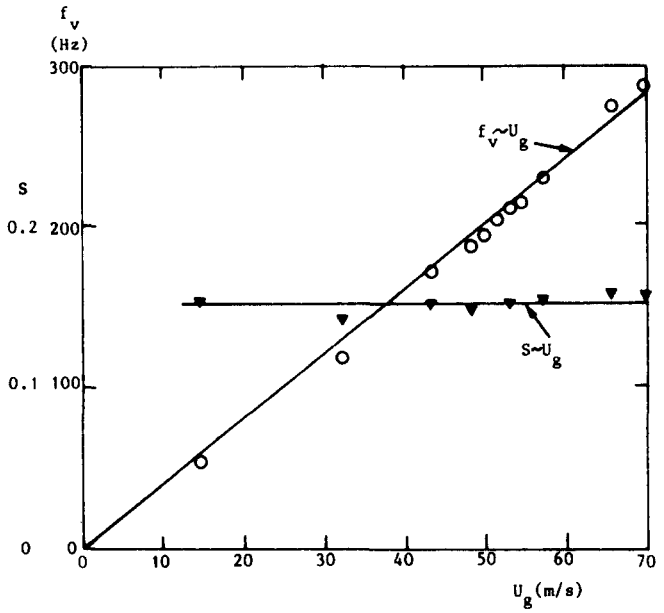

(a) Frequency and Strouhal number versus U_g

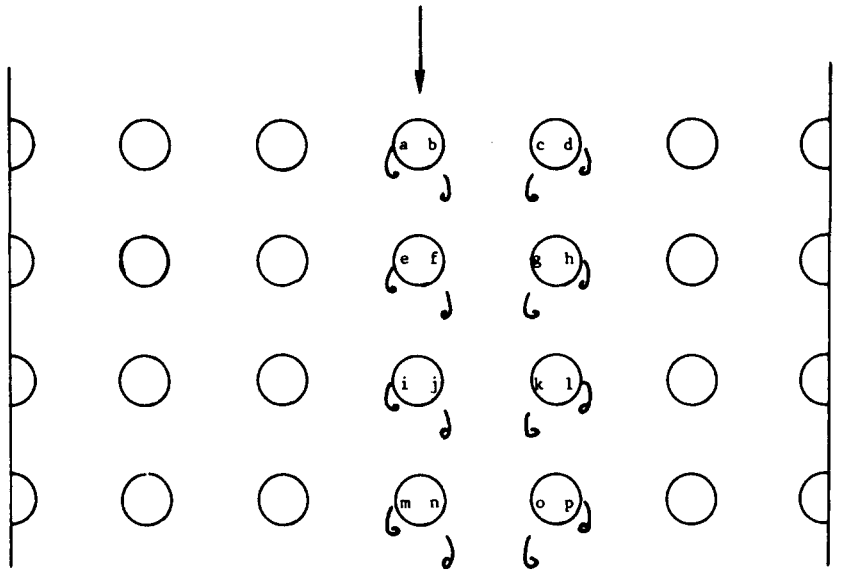

(b) Simulated shedding pattern of vortex shedding

Figure 15 Experimental results for in-line tube bank with four rows for $P_T/d=2.67$ and $P_L/d=2.31$

C_L curves are compared with those of the staggered tube bank (Figure 12), it will be seen that the pattern is quite different and, especially, that the results for rows 2, 3, and 4 are almost identical, confirming the previous conclusion of a periodic vortex wake correlated with each line of tubes. This notion is further confirmed by the fluctuating pressures shown in Figure 17, which are almost identical for rows 2, 3, and 4. On the other hand both C_L and C'_p show completely different behaviors for row 1, which are almost indistinguishable from those exhibited by the staggered tube bank. Apart from a greater degree of Reynolds number sensitivity, the average pressure distribution curves for row 1 (Figure 18) are also close to those for the staggered tube row (Figure 13). We may then conclude from this that the flow pattern previously surmised for row 1 (Figure 15) is probably incorrect and that the general flow regime produced by the first row of the two tube banks is largely uninfluenced by the radically differing geometries of the downstream rows of tubes. If this is so, one would expect the major difference in flow regime to be initiated in row 2 and to be dramatically different for these two extremes of geometry.

Although there was no noticeable difference between the fluctuating pressures measured on rows 2, 3, and 4 to identify some major event occurring in row 2, as we have already pointed out, such evidence was revealed from the average pressure plots shown in Figure 18. The most worrying feature of $C_{p_{av}}$ for row 2 is the implication that the average static pressure over the range $0° < \theta < 70°$ exceeded the stagnation pressure, which one might expect to record at $\theta = 0°$. In an unsteady flow

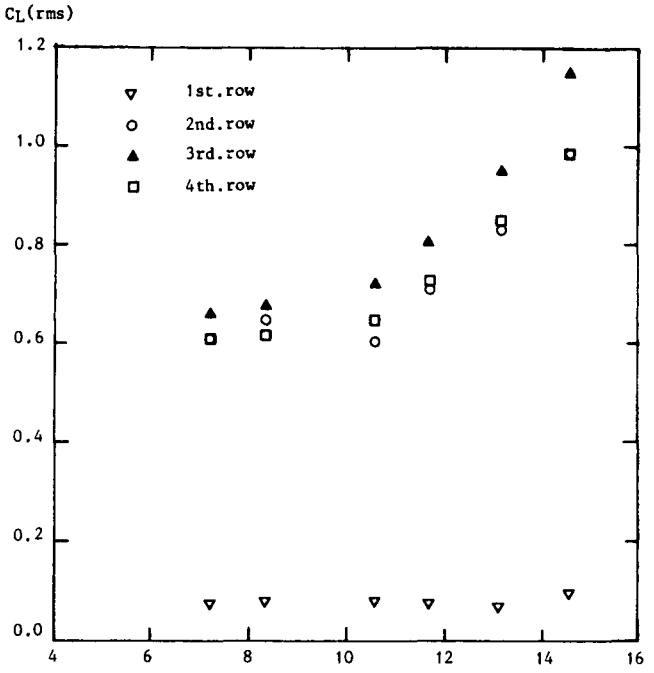

Figure 16 Graph of the rms value of the total lift coefficient C_L versus U_g for in-line tube bank of four rows with $P_T/d=2.67$ and $P_L/d=2.31$

it is possible that stagnation pressure could increase moving downstream due to dq/dt, and there is evidence of such slight increases also in rows 3 and 4. However, the results measured for row 2 are so extraordinary that they should be confirmed by further research to the in-line tube bank case. Having said that, the general trends for rows 2 and 4 are such as one might expect regarding the shielding effect which results from downstream alignment of the tubes, namely very much less wake energy loss and consequent static depression on the tube rear faces. It would seem that row 2 was most influenced in this respect. It is felt that more detailed investigations of these flows would be extremely helpful toward obtaining a clearer understanding of the fluid dynamic activity in the first two rows of tube banks, although one must bear in mind that failures due to excitation more frequently occur in the second rows of different types of heat exchangers.

Modified staggered tube bank with offset third row

The aim of this experiment was to investigate the effect of disturbing the symmetry of the staggered tube bank by displacing all tubes of the third row transversely through a distance of 1 in. The modified tube bank geometry is shown in Figure 19. Under these conditions it was anticipated that the regular vortex shedding pattern of Figure 10 would be destroyed. Attention was focused upon the upstream and downstream effects experienced by rows 2 and 4.

Measured values of the rms fluctuating lift coefficients for the second and fourth rows are shown in Figure 20 in comparison with those which were found for the original symmetrically staggered tube bank. Both second and fourth rows experienced a remarkable drop in the level of C_L by about 80% and 50%, respectively. It is clear that departure from symmetry in the third row had disrupted the normal vortex shedding processes in the second and fourth rows, presumably by disturbing the periodicity in the wake of row 2 and therefore of the incident flow upon wake 4. Row 2, always the most vulnerable for tube failures, was more strongly influenced than row 4, and the resulting values of C_L were almost identical and extremely low.

Conclusions

The following conclusions may be drawn from this investigation.

(a) In the symmetrically staggered tube bank it was found that the second row produced the highest levels of C_L, which increased from about 0.6 at $Re=1.5\times10^4$ to 1.0 at $Re=3.2\times10^4$. For this in-line tube bank, the second, third, and fourth rows had relatively close levels of C_L in the range $Re=1.8\times10^4$ to 3.7×10^4, increasing from about 0.66 to 1.08. In both tube banks the first row experienced remarkably low levels of C_L compared with downstream rows. Surface pressure measurements confirmed that this was due to almost uniform values of fluctuating pressure coefficient, C'_p, around the tube.

(b) The combined evidence of hot wire measurements (indicating vortex patterns), fluctuating pressures, and C_L values led to the conclusion that the flow behaviors in rows 2, 3, and 4 are quite similar in the in-line tube bank but are remarkably different in the staggered tube bank.

(c) It was found that the technique of displacing row 3 transversely to destroy symmetry in the staggered tube bank led to dramatic reductions of exciting forces in rows 2 and 4. The C_L values were in the range 0.19 and 0.23 for Re values from 2.3×10^4 to 3.2×10^4, being almost identical for both rows. Compared with the symmetrically staggered case this represented a reduction of C_L of 80% for row 2 and 50% for row 4. The use of irregular geometries in staggered tube banks ought therefore to be investigated more fully, as it seems to offer a simple solution to the reduction of aerodynamic excitations and vibrations associated with vortex shedding in heat exchanger tube banks.

Acknowledgments

The authors wish to express their thanks to Miss Roberta Stocks for her assistance in producing this manuscript. Dr. R. S. Hill died in August 1985, after the completion of this work, and his coauthors wish to acknowledge his brilliance in experimental research and his many outstanding contributions to the study of aerodynamic excitation in heat exchangers.

References

1 Tritton, D. J. Experiments on the flow past a circular cylinder at a low Reynold's number. *J. Fluid Mech.*, 1959, **6**, 547–567
2 Humphreys, J. S. On a circular cylinder in a steady wind at transition Reynold's number. *J. Fluid Mech.*, 1960, **9**, 603–612
3 Keefe, R. T. An investigation of the fluctuating forces acting on a stationary circular cylinder in a subsonic stream and of the associated sound field. UTIA Report No. 76, 1961
4 Fung, C. Y. Fluctuating lift and drag acting on a cylinder in a flow at supercritical Reynold's numbers. *J. Aero. Sci.*, 1960, **27**, No. 11
5 Schmidt, L. V. Fluctuating force measurements upon a circular cylinder at Reynold's numbers up to 5×10^6. NASA-TM-X-57779, 1966, 19.1–19.17
6 McGregor, D. M. An experimental investigation of the oscillating pressures on a circular cylinder in a fluid stream. University of Toronto, UTIA TN 14, 1957
7 Kacker, S. C., Pennington, B., and Hill, R. S. Fluctuating lift coefficient for a circular cylinder in a cross flow. *J. Mech. Eng. Sci.*, 1974, **16**, No. 4

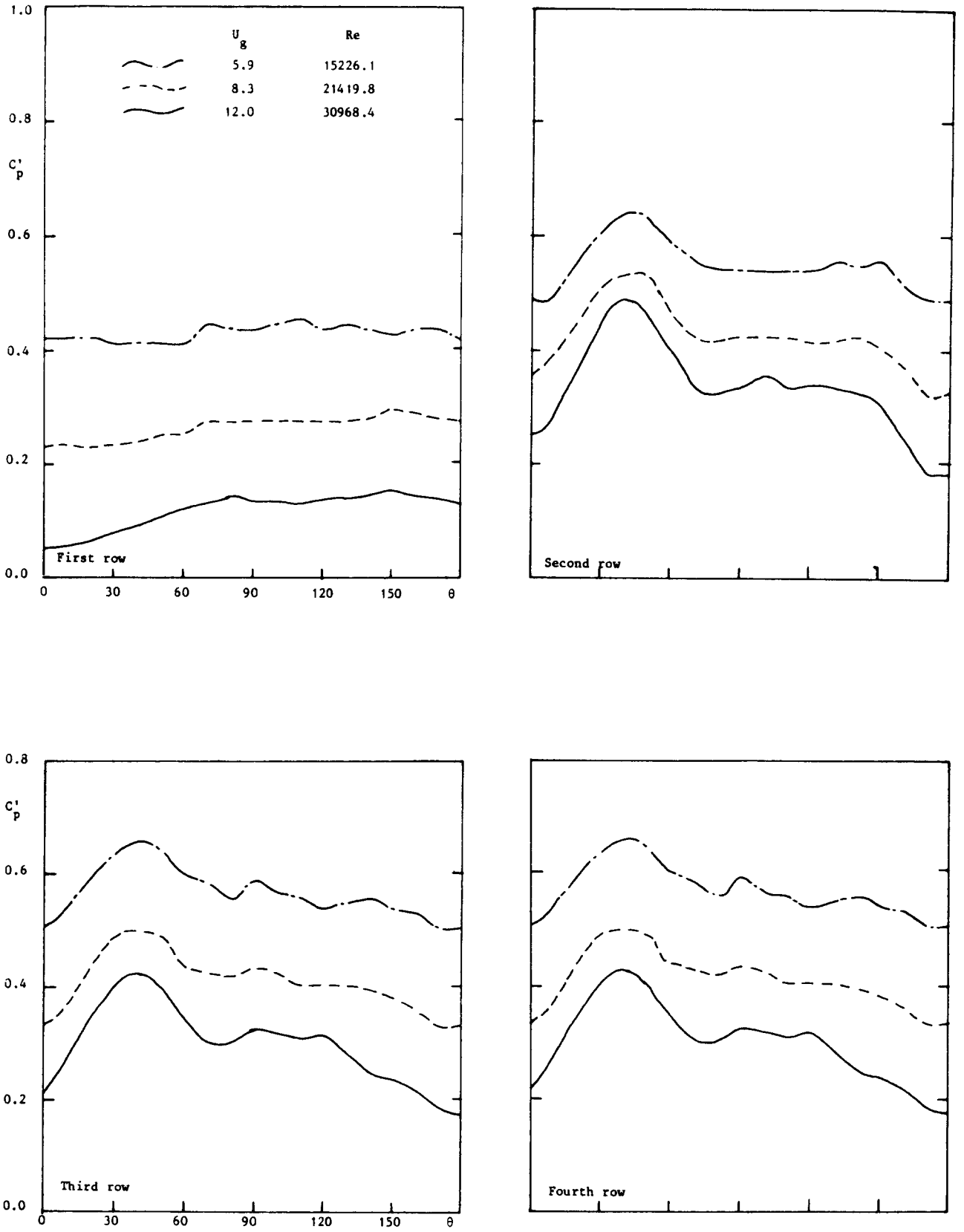

Figure 17 Fluctuating pressure distribution for in-line tube bank of four rows with $P_T/d=2.67$ and $P_L/d=2.31$

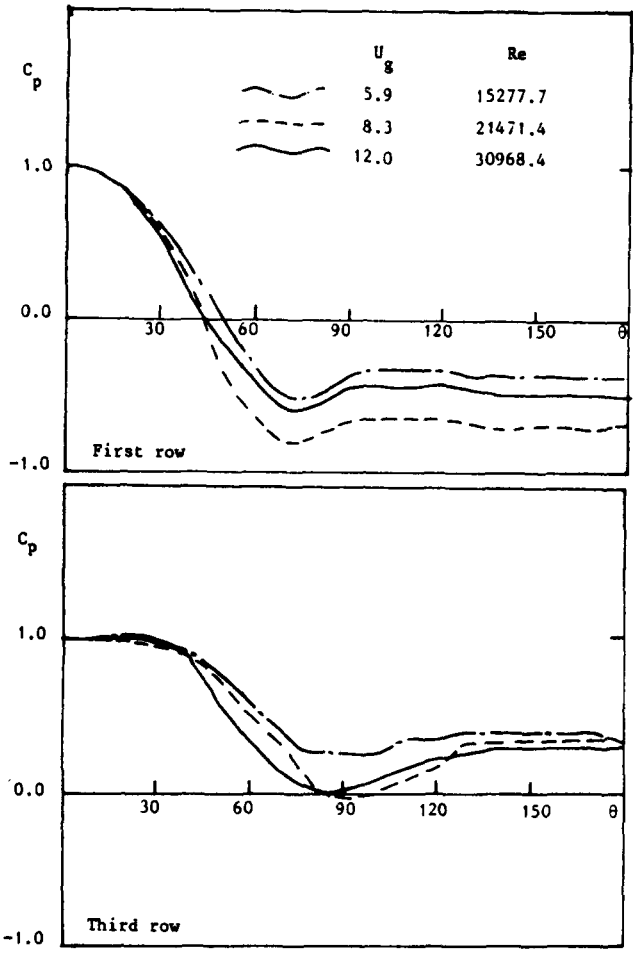

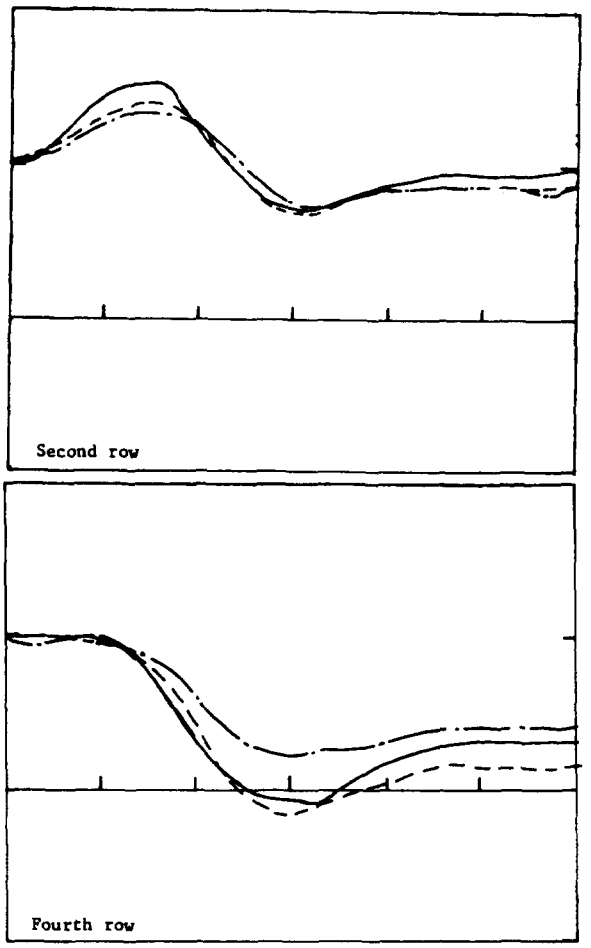

Figure 18 Steady pressure distribution for in-line tube banks of four rows with P_T/d=2.67 and P_L/d=2.31

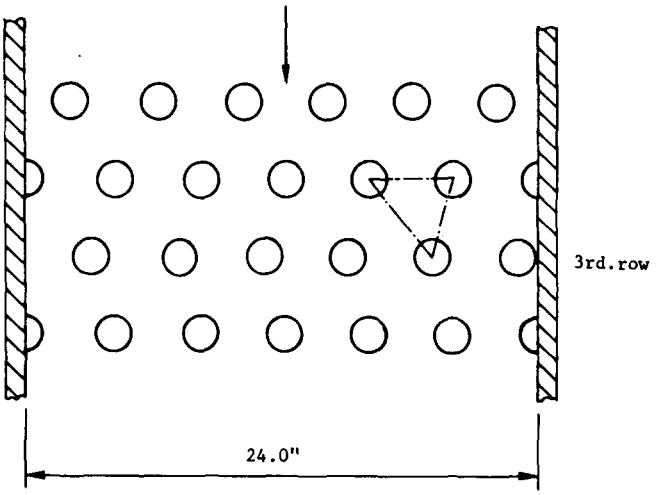

Staggered tube bank of P_T/d = 2.67 and P_L/d = 2.31 with all tubes in the third row shifted by 1" in the perpendicular direction to the stream.

Figure 19 Modified staggered tube bank for additional investigation

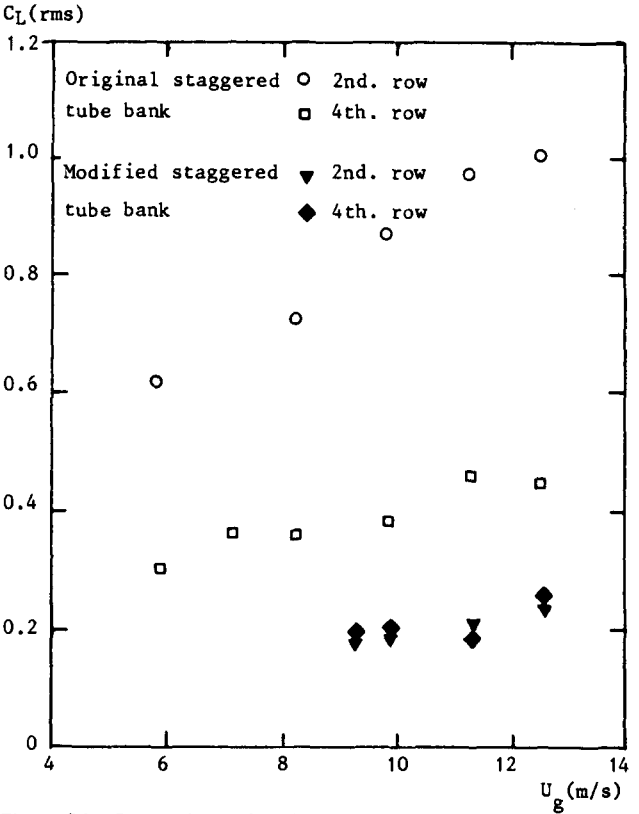

Figure 20 Comparison of C_L between the original staggered tube bank and the modified staggered tube bank

8 Lewis, R. I. and Shim, K. C. Vortex cloud analysis of the average and fluctuating flow past a cylinder in a uniform stream. Int. Seminar on Engineering Applications of the Surface and Cloud Vorticity Methods, Technical University of Wroclaw, Poland, Conf. No. 9, April 1986

9 Chen, Y. N. Fluctuating lift forces of the Kármán vortex streets on single circular cylinders and in tube bundles. Part III: Lift forces in tube bundles. *J. Eng. Industry*, 1972, 623

10 Batham, J. P. Pressure distributions on in-line tube arrays in cross flow. Int. Symp. on Vibration Problems in Industry, Keswick, 1973

11 Pennington, B. On fluctuating phenomena associated with circular cylinders in cross flow. Ph.D. Thesis, University of Newcastle Upon Tyne, 1973

12 Shim, K. C. Fluctuating phenomena in tube banks in cross-flow. Ph.D. Thesis, University of Newcastle Upon Tyne, 1985

13 Hill, R. S., Shim, K. C., and Lewis, R. I. Source of excitation in tube banks due to vortex shedding. *Proc. I.Mech.E.*, **200**, C4, 1986, 293–301

14 Chen, Y. N. Fluctuating lift forces of the Kármán vortex streets on single cylinders and in tube bundles. Part II: Lift forces on single cylinder. *J. Eng. Industry*, 1972, 613

15 Gerrard, J. H. An experimental investigation of the oscillating lift and drag of a circular cylinder shedding turbulent vortices. *J. Fl. Mech.*, 1962, **11**, 244–256